Native-oxide defined ring contact for low threshold vertical-cavity lase

D. L. Huffaker, D. G. Deppe, and K. Kumar
Microelectronics Research Center, Department of Electrical and Computer Engineering, The University of Texas at Austin, Austin, Texas 78712-1084

T. J. Rogers
Martin Marietta Laboratories–Syracuse, Syracuse, New York 13121

(Received 4 February 1994; accepted for publication 1 April 1994)

Data are presented characterizing a new process for fabrication of vertical-cavity surface-emitting lasers based on the selective conversion of high Al composition epitaxial AlGaAs to a stable native oxide using "wet oxidation." The native oxide is used to form a ring contact to the laser active region. The resulting laser active regions have dimensions of 8, 4, and 2 μm. The lowest threshold laser is achieved with the 8-μm active region, with a minimum threshold current of 225-μA continuous wave at room temperature.

It is well appreciated that high Al composition single-crystal AlGaAs is chemically unstable in the typical room-temperature atmospheric environment, and "hydrolyzes" into various oxides in times ranging from minutes to months or years.[1] This chemical instability can be deleterious to the performance of semiconductor devices which use the AlGaAs material. On the other hand, Holonyak and a variety of co-workers have developed a process whereby at elevated temperatures the chemical instability of high Al composition AlGaAs leads to the conversion of this material to stable "native" oxides of Al_xO_y.[2–5] An advantage of the oxidation process for III-V devices is that the high Al composition AlGaAs may be selectively oxidized as compared to lower Al composition AlGaAs, especially as compared to GaAs. This selectivity makes it possible to "bury" the oxidized layers, using lateral diffusion, below single-crystal GaAs layers.[3–5] We use this characteristic to form a ring contact to a vertical-cavity surface-emitting laser (VCSEL).

One of the attractive features about the VCSEL is its potential for low lasing threshold. This potential stems directly from the ability to minimize the active volume using the short, low-loss vertical cavity. The potential for low threshold current, along with single spectral mode lasing, good beam characteristics, and surface normal emission, makes the VCSEL an important device to consider for integrated optoelectronic applications. Earlier work has already been reported in which submilliampere threshold currents were achieved,[6,7] and more recently room-temperature continuous wave (cw) thresholds as low as 470 μA have been reported.[8] In this letter we report even lower threshold currents for devices which utilize the native-oxide process, with a minimum threshold current of 225 μA demonstrated for an 8-μm square device.

Figure 1 shows a schematic cross section representing the epitaxial layers of the VCSEL after oxidation. The epitaxial structure is grown on a GaAs substrate by molecular beam epitaxy (MBE) and consists of a 0.5-μm n-type GaAs buffer layer followed by a 26 pair, n-type AlAs/GaAs quarter-wave distributed Bragg reflector, an active region consisting of three 60-Å $In_{0.2}Ga_{0.8}As$ quantum wells separated by 100-Å GaAs barriers in a one-wavelength-thick GaAs spacer layer, and followed by one pair of quarter-wavelength layers of p-type AlAs/GaAs. A seven-period graded superlattice is used on both sides of the AlAs layers immediately surrounding the active region, which is effective in reducing the electrical series resistance.

After the MBE growth of the heterostructure, the lasers are fabricated by first defining 30- or 60-μm-diam photoresist dots on the p-type GaAs surface. The exposed p-type GaAs layer is then selectively removed to form shallow GaAs mesas using a succinic acid solution maintained at a temperature of 50 °C with the pH adjusted to 4.3.[9] After removing the photoresist from the GaAs mesas, the exposed AlAs layer is oxidized in a furnace set at 475 °C. The oxidation time is ~3 min. As described in the initial papers on the hydrolyzation process,[2–5] the furnace is supplied with a flow of N_2 bubbled through de-ionized water heated to a temperature of 95 °C. The oxidation of the AlAs layer proceeds laterally beneath the GaAs mesas due to diffusion. This buried oxide layer then defines a current path for carrier injection through the remaining intact p-type AlAs into the laser active region (see Fig. 1).

Figure 2 shows a scanning electron microscope photograph looking down at the top surface of the epitaxial structure after oxidation. The buried oxide shown in Fig. 2 forms a 4 μm×4 μm square region which serves as the current injection path. The square pattern formed by oxidation is indicative that the process has a crystallographic preference. From our studies of other heterostructures we have found that the resulting square geometry due to the oxidation is directly attributable to the graded superlattice layers grown

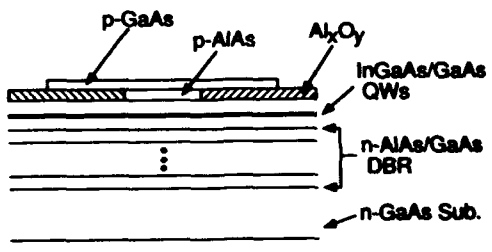

FIG. 1. Schematic cross section (not to scale) of the buried ring contact VCSEL structure showing the role of the lateral oxidation of the AlAs underneath the GaAs mesa in defining the device active region.

 0003-6951/94/65(1)/97/3/$6.00

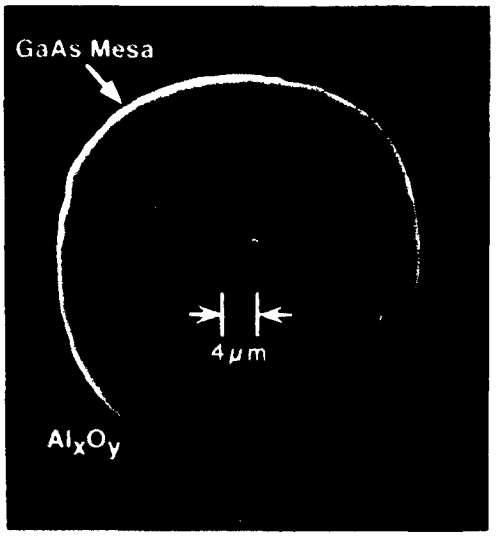

FIG. 2. Scanning electron microscope photograph of a native-oxide defined 4-μm square AlAs region buried beneath a 30-μm-diam GaAs mesa. The oxide layer surrounding and beneath the GaAs mesa provides device isolation for current injection.

during MBE between the GaAs and AlAs. A circular dot shape results even for submicron dimensions for the lateral oxidation of very similar heterostructures in which the graded interfaces are absent.

The 30-μm GaAs mesas are defined with 500-μm spacings, and electrical isolation between the laser devices is also provided by the exposed Al_xO_y layer. Electrical contact is made to the p-type GaAs surface and exposed Al_xO_y using Cr/Au metallization. The active areas of the laser are exposed using a lift-off process to remove metallization, forming a 10-μm-diam opening above the active region. The lift-off leaves 100 μm$\times$400 μm rectangular contact pads around each device aligned on the 500 μm$\times$500 μm grid. The top reflectors,which are an additional five pairs of quarter-wave ZnSe/CaF_2 layers, are then deposited on the p side using electron-beam evaporation. The ZnSe/CaF_2 materials have been shown to form high reflectivity, low-loss mirrors,[10,11] and possess advantages over the lower contrast AlAs/GaAs mirrors. Two advantages are the flexibility of probe wavelengths in optical addressing schemes,[12,13] and the reduction of the lateral mode for small active volume lasers.[14]

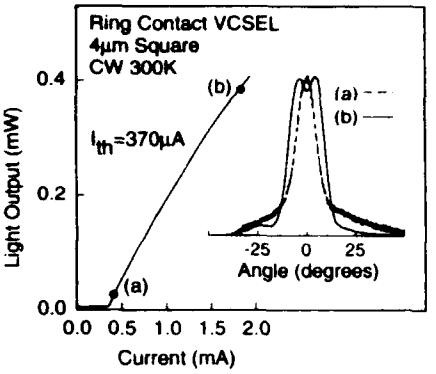

FIG. 4. Light vs current curve measured cw at room temperature for a 4-μm square VCSEL. The inset shows measured far-field radiation patterns at current levels of (a) 400 μA (dashed curve) and (b) 2.0 mA (solid curve).

Figures 3 through 5 show the light versus current characteristics and far-field radiation patterns for the native-oxide defined lasers with active regions of 8-, 4-, and 2-μm squares, respectively. The lowest threshold currents are achieved for 8-μm square devices, with a minimum cw threshold of 225 μA along with an output power of 0.46 mW at six times threshold (Fig. 3). The far-field radiation pattern remains a stable single lobe up to two times threshold, at which point side lobes appear. Also shown in Fig. 3 is the far-field radiation pattern at four times threshold with the side lobes evident.

Despite the low threshold current achieved in the 8-μm device, there is some leakage current due to the oxidation process which degrades the p-n junction. We speculate that this leakage current is stress induced by the oxide, and the problem becomes more severe for smaller device sizes. This leakage current is at least partly responsible for the increased threshold currents measured for the smaller active regions of 4 μm (Fig. 4) and 2 μm (Fig. 5). Comparison of the current-voltage characteristics on the three different device sizes show increasing forward current for a given voltage as the device diameter is decreased (data not shown). We have

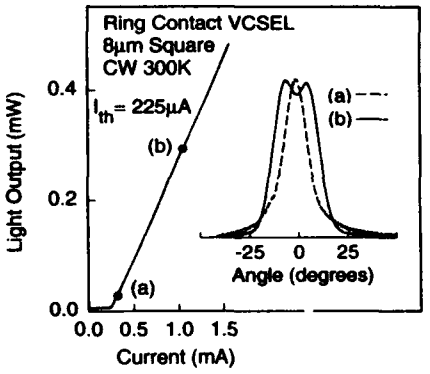

FIG. 3. Light vs current curve measured cw at room temperature for an 8-μm square VCSEL. The inset shows measured far-field radiation patterns at current levels of (a) 280 μA (dashed curve) and (b) 1.0 mA (solid curve).

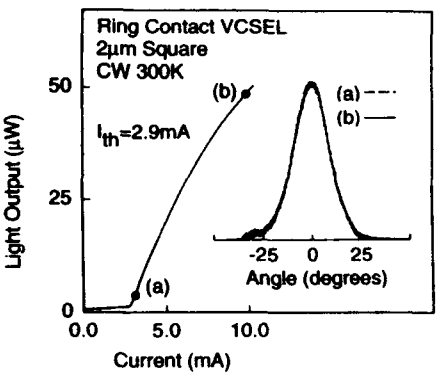

FIG. 5. Light vs current curve measured cw at room temperature for a 2-μm square VCSEL. The inset shows measured far-field radiation patterns at current levels of (a) 3.0 mA (dashed curve) and (b) 10 mA (solid curve).

found that the leakage current through the oxide is negligible, and again speculate that the leakage current arises due to minority carrier recombination at the oxide-semiconductor interfaces. If this leakage current is controlled, we expect threshold currents to scale with decreasing active area at least to the 4-μm dimension. An estimate of the lasing mode diameter from the threshold far-field radiation patterns suggests that the lasing mode is on the order of ~3–4 μm diameter in both the 8- and 4-μm devices, and therefore is well confined. In the smaller area devices the lasing mode is more stable, and remains single lobed up to four times threshold for the 4-μm square, at which point side lobes appear (see Fig. 4). The radiation pattern of the 2-μm square device, Fig. 5, shows an increased angular width due to the reduced active region, and remains single lobed over the range of measurement.

An inherent problem in VCSEL designs in which the hole current must pass through p-type semiconductor Bragg reflectors is high electrical series resistance. While there has been progress in reducing the mirror resistance through graded heterojunctions and localized doping, as the device dimensions continue to scale smaller this resistance problem will become more severe. An advantage of the buried native oxide in forming the ring contact to the VCSEL is that the hole current must pass through only one p-type heterojunction before injection into the active region. The 8-μm native-oxide defined laser, which shows little leakage current, has a threshold voltage drop of 1.9 V, with a voltage drop of 2.9 V at four times threshold.

In summary, we have presented a new process for the fabrication of VCSELs based on a native-oxide defined ring contact. Using this process we have demonstrated a low cw room-temperature lasing threshold of 225 μA. Since the native-oxide process is nearly planar, provides good electrical isolation, and does not require complex epitaxial regrowth, it should be useful for integrated optoelectronic circuits incorporating the VCSEL as well as for the discrete laser diodes demonstrated here.

The authors acknowledge useful conversations with N. Holonyak, Jr. concerning the oxidation of AlGaAs, and are also grateful to J. Sarathy and J. C. Campbell for assistance during this work. TJR acknowledges useful conversations with L. F. Lester. The work at the University of Texas at Austin has been supported by the Office of Naval Research under Contract No. N-0014-91-J-1952, the Joint Services Electronics Program under Contract No. F49620-92-C-0027, and the Texas Advanced Technology Program under Contract No. TP-024.

[1] J. M. Dallesasse, N. El-Zein, N. Holonyak, Jr., K. C. Hsieh, R. D. Burnham, and R. D. Dupuis, J. Appl. Phys. **68**, 2235 (1990).
[2] J. M. Dallesasse, N. Holonyak, Jr., A. R. Sugg, T. A. Richard, and N. El-Zein, Appl. Phys. Lett. **57**, 2844 (1990).
[3] A. R. Sugg, E. I. Chen, T. A. Richard, N. Holonyak, Jr., and K. C. Hsieh, Appl. Phys. Lett. **62**, 1259 (1993).
[4] A. R. Sugg, E. I. Chen, T. A. Richard, N. Holonyak, Jr., and K. C. Hsieh, J. Appl. Phys. **74**, 797 (1993).
[5] S. A. Maranowski, A. R. Sugg, E. I. Chen, and N. Holonyak, Jr., Appl. Phys. Lett. **63**, 1660 (1993).
[6] R. S. Geels and L. A. Coldren, Appl. Phys. Lett. **57**, 1605 (1990).
[7] T. Wipiejewski, K. Panzlaff, E. Zeeb, and K. J. Ebeling, IEEE Photon. Technol. Lett. **5**, 889 (1993).
[8] C. C. Hansing, H. Y. Deng, D. L. Huffaker, D. G. Deppe, B. G. Streetman, and J. Sarathy, IEEE Photon. Technol. Lett. **6**, 320 (1994).
[9] A. J. Tang, K. Sadra, and B. G. Streetman, J. Electrochem. Soc. **140**, L82 (1993).
[10] C. Lei, T. J. Rogers, D. G. Deppe, and B. G. Streetman, J. Appl. Phys. **69**, 7430 (1991).
[11] T. J. Rogers, C. Lei, D. G. Deppe, and B. G. Streetman, Appl. Phys. Lett. **62**, 2027 (1993).
[12] T. Numai, M. Sugimoto, I. Ogura, H. Kosaka, and K. Kasahara, Appl. Phys. Lett. **58**, 1250 (1991).
[13] D. L. Huffaker, W. D. Lee, D. G. Deppe, C. Lei, T. J. Rogers, J. C. Campbell, and B. G. Streetman, IEEE Photon. Technol. Lett. **3**, 1064 (1991).
[14] D. L. Huffaker, C. C. Lin, D. G. Deppe, B. G. Streetman, and T. J. Rogers, IEEE Photon. Technol. Lett. **6**, 135 (1994).